2.1 Introduction

In this chapter general properties of the radiation fields at accelerators will be discussed. To do this, the concept of particle yield and solid angle will be introduced. Following that, a theoretical approach to particle transport will be introduced. The Monte Carlo technique will be described and illustrated by simple examples. The manipulation of charged particles using electromagnetic fields will be reviewed due to its importance for understanding the handling of the accelerated beams.

2.2 Primary Radiation Fields at Accelerators-General Considerations

Accelerated charged particles, except for the singular pnenonemon of synchrotron radiation that will be discussed in Section 3.2.3, do not produce radiation unless there is some interaction with matter. The charged particles directly accelerated, and otherwise manipulated by the electromagnetic fields within the accelerator, are referred to as the **primary** particles or beam. All other particles that are produced from this beam either due to the interactions of these primary particles in matter or due to synchrotron radiation are referred to as **secondary** particles. In some instances, one finds references to **tertiary** particles that result from the interactions in matter of the secondary particles or are emitted in their radioactive decay. Confusion at many high energy accelerators sometimes arises from the fact that secondary and tertiary particles and ions can now be collected into beams of their own and even accelerated. In these instances, when the secondary or tertiary particles are employed at some location separated from the place where they were initially produced, they can obviously play the role of a primary particle.

If one considers primary particles incident upon a physical object such as a target, the **yield**, Y, of secondary particles is a crucial parameter. The yield is typically a function of both angle and particle energy and is defined according to Fig. 2.1. Scattered reaction products are found at a "point of interest" located at radius, r, and polar angle, θ, relative to the direction of the incident particle along the positive z -axis. In general, particle **differential yields** are expressed in terms of particles per unit solid angle at the point of interest and are commonly normalized to the number of incident particles or to the beam current or total delivered charge. Such particle yields, dependent upon both target material and thickness, are reported in terms of particle type, energy, and angular distributions. The rate of production of the desired reaction products and their energy spectra is, in general, a strong function of both θ and the incident particle energy E_o. There is usually no dependence on the azimuthal angle in a spherical coordinate system.[1]

[1]The single exception is the case in which the spins of the target nuclei and/or the incident particle are oriented along some chosen direction in a "polarization" experiment.

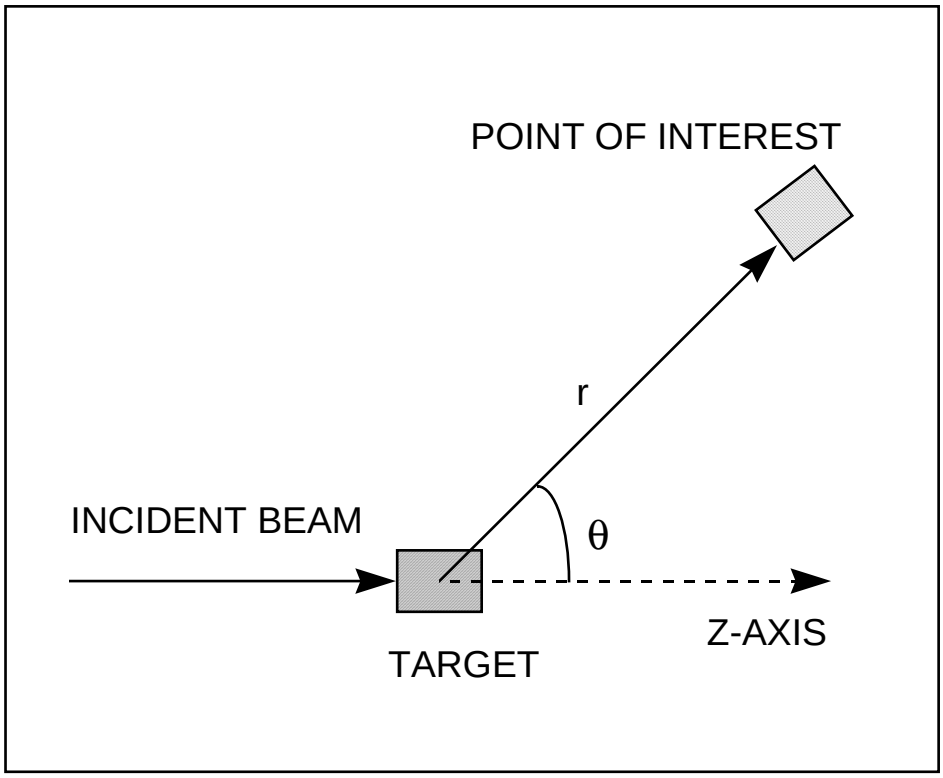

Fig. 2.1 Conceptual interaction of incident beam with material (target) which produces radiation at the point of interest located at polar coordinates (r, θ).

In principle, the particle yield could be obtained directly from differential cross sections for given incident particle kinetic energy E,

$$\frac{d\sigma(\theta, E)}{d\Omega},$$

where $\sigma(\theta, E)$ is the cross section as a function of energy and angle and Ω is the solid angle into which the secondary particles are produced. Y could, in principle be obtained from an integration of this cross section as it varies while the incident particle passes through the target material.

Calculations of the radiation field that directly use the cross sections are often not practical because targets hit by beam are not really thin. Thus one cannot ignore energy loss or secondary interactions in the target. Furthermore, the knowledge of cross sections at all energies is generally incomplete with the unfortunate result that one cannot always integrate over θ and E to get the total yield.

For many applications, the details of the angular distributions **of total secondary particle yield**, $dY(\theta)/d\Omega$, and the **angular dependence of the emitted particle energy spectrum**, $d^2Y(\theta,E)/dEd\Omega$, are very important.

Often, the particle fluence is needed at a particular location at coordinates (r,θ) from a known point source of beam loss while the angular distributions of $dY/d\Omega$ are generally expressed in units of particles/(steradian-incident particle). To obtain the total fluence $\Phi(\theta)$ [e.g., particles/(cm^2·incident particle)], or differential fluence $d\Phi(\theta,E)/dE$ [e.g., particles/(cm^2·MeV·incident particle)] at a given distance r (cm) at a specified angle θ from such a **point source**[2], one must simply multiply the yield values by r^{-2} (e.g., cm^{-2}):

$$\Phi(\theta) = \frac{1}{r^2}\frac{dY(\theta)}{d\Omega} \quad \text{and} \quad \frac{d\Phi(E,\theta)}{dE} = \frac{1}{r^2}\frac{d^2Y(E,\theta)}{dEd\Omega}. \tag{2.1}$$

Given the fact that secondary, as well as primary, particles can create radiation fields, it is quite obvious that the transport of particles through space and matter can become a very complex matter. In the following section, the advanced techniques for handling these issues are described.

2.3 Theory of Radiation Transport

The theoretical material in this section is largely due to the work of O'Brien (OB80). It is included to show clearly the mathematical basis of the contents of shielding codes, especially those that use the Monte Carlo method. Vector notation is used in this section.

2.3.1 General Considerations of Radiation Transport

Stray and direct radiations at any location are distributed in particle type, direction, and energy. To determine the amount of radiation present for radiation protection purposes we must assign a magnitude to this multidimensional quantity. This is done by forming a double integral over energy and direction of the product of the flux and an approximate dose equivalent per unit fluence conversion factor, summed over particle type;

$$H(\vec{x},t) = \sum_i \oint_{4\pi} d\vec{\Omega} \int_0^\infty dE\ f_i(\vec{x},E,\vec{\Omega},t) P_i(E), \tag{2.2}$$

where the summation index i is over the various particle types, $\vec{\Omega}$ is the direction vector of particle travel, $\vec{x}$ is the coordinate vector of the point in space where the dose or dose equivalent is to be calculated, E is the particle energy, t is time, and i is the particle type. $P_i(E)$ is the dose equivalent per unit fluence conversion factor expressed as a function of energy and particle type for the i^{th} particle. The inner integral is over all energies while the outer integral is over all spatial directions from which contribute to the radiation field at the location specified by $\vec{x}$. The result of the integration is H, the dose or dose

[2] A point source is one in which the dimensions of the source are small compared with the distance to some other location of interest.

equivalent rate at location $\vec{x}$ and time *t*. Values of $P_i(E)$ are given in Figs. 1.4, 1.5, and 1.6. The angular flux, $f_i(\vec{x},E,\vec{\Omega},t)$, the number of particles of type *i* per unit area, per unit energy, per unit solid angle, per unit time at location $\vec{x}$, with a energy *E*, at a time *t* and traveling in a direction $\vec{\Omega}$ is related to the flux density, $\phi_i(\vec{x},t)$, by integrating over direction,

$$\phi_i(\vec{x},t) = \sum_i \oint_{4\pi} d\vec{\Omega} \int_0^\infty dE\ f_i(\vec{x},E,\vec{\Omega},t)\,. \tag{2.3}$$

The angular flux, $f_i(\vec{x},E,\vec{\Omega},t)$, is connected to the fluence $\Phi_i(\vec{x})$ by integrating over the intervening period of time (t_i to t_f),

$$\Phi_i(\vec{x}) = \oint_{4\pi} d\vec{\Omega} \int_0^\infty dE \int_{t_i}^{t_f} dt\ f_i(\vec{x},E,\vec{\Omega},t)\,, \tag{2.4}$$

and to the energy spectrum at point $\vec{x}$ at time *t* by,

$$\phi_i(\vec{x},t,E) = \oint_{4\pi} d\vec{\Omega}\ f_i(\vec{x},E,\vec{\Omega},t)\,. \tag{2.5}$$

To determine the proper dimensions and composition of a shield, the amount of radiation, expressed in terms of the dose or dose equivalent, which penetrates the shield and reaches locations of interest must be calculated. This quantity must be compared with the maximum permissible dose equivalent. If the calculated dose equivalent is too large, either the conditions associated with the source of the radiation or the physical properties of the shield must be changed. The latter could be a change in shield materials, dimensions, or both. If the shield cannot be adjusted, then the amount of beam loss allowed by the beam control instrumentation, the amount of residual gas in the vacuum system, or the amount of beam accelerated may have to be reduced. It is difficult and expensive, especially in the case of the larger accelerators, to alter permanent shielding or operating conditions if the determination of shielding dimensions and composition has not been done correctly. The methods for determining these quantities have been investigated by a number of workers. The next section only summarizes the basics of this important work.

2.3.2 The Boltzmann Equation

The primary tool for determining the amount of radiation reaching a given location is the *stationary form* of the Boltzmann equation (henceforth, simply the Boltzmann equation) which, when solved, yields the angular flux, f_i, the distribution in energy and angle for each particle type as a function of position and time. The angular flux is then converted to dose equivalent by means of Eq. (2.2). This section describes the theory that yields the

distribution of radiation in matter, and discusses some of the methods for extracting detailed numerical values for elements of this distribution such as particle flux, or related quantities, such as dose, activation or instrument response. The basis for this theory is the Boltzmann equation, a statement of all the processes that the particles of various types, including photons, that comprise the radiation field can undergo.

The Boltzmann equation is an integral-differential equation describing the behavior of a dilute assemblage of corpuscles. It was derived by Ludwig Boltzmann in 1872 to study the properties of gases but applies equally to the behavior of those "corpuscles" which comprise ionizing radiation. This equation is a continuity equation of the angular flux, f_i, in phase space which is made up of the three space coordinates of Euclidian geometry, the three corresponding direction cosines, the kinetic energy, and the time. The density of radiation in a volume of phase space may change in five ways:

- **Uniform translation**; where the spatial coordinates change, but the energy-angle coordinates remain unchanged;

- **Collisions**; as a result of which the energy-angle coordinates change, but the spatial coordinates remain unchanged, or the particle may be absorbed and disappear altogether;

- **Continuous slowing down**; in which uniform translation is combined with continuous energy loss;

- **Decay**; where particles are changed through radioactive transmutation into particles of another kind; and

- **Introduction**; involving the direct emission of a particle from a source into the volume of phase space of interest: electrons or photons from radioactive materials, neutrons from an α-n emitter, the "appearance" of beam particles, or particles emitted from a collision at another (usually higher) energy.

Combining these five elements yields

$$\tilde{\mathrm{B}}_i f_i(\vec{x}, E, \vec{\Omega}, t) = Q_{ij} + Y_{ij} \tag{2.6}$$

where the mixed differential and integral **Boltzmann operator** for particles of type i, $\tilde{\mathrm{B}}_i$, is given by

$$\tilde{\mathrm{B}}_i = \vec{\Omega} \cdot \nabla + \sigma_i + d_i - \left\{ \frac{\int dE}{\int E dE} \right\} S_i \,, \tag{2.7}$$

$$Q_{ij} = \sum_j \oint_{4\pi} d\vec{\Omega}' \int_o^{E_{\max}} dE_B \sigma_{ij}\left(E_B \to E, \vec{\Omega}' \to \vec{\Omega}\right) f_j(\vec{x}, E, \vec{\Omega}', t)\,, \tag{2.8}$$

and

$$d_i = \frac{\sqrt{1-\beta_i^2}}{\tau_i \beta_i c}\,. \tag{2.9}$$

In Eq. (2.7);

Y_i is the number of particles of type i introduced by a source per unit area, time, energy, and solid angle;

σ_i is the absorption cross section for particles of type i. To be dimensionally correct, this is actually the *macroscopic* cross section or linear absorption coefficient $\mu = N\sigma$ as defined in Eq. (1.8);

d_i is the decay probability per unit flight path of radioactive particles (such as muons or pions) of type i ;

S_i is the stopping power for charged particles of type i (assumed to be zero for uncharged particles);

Q_{ij} is the "scattering-down" integral, the production rate of particles of type i with a direction $\vec{\Omega}$, an energy E at a location $\vec{x}$, by collisions with nuclei or decay of j -type particles having a direction $\vec{\Omega}'$ at a higher energy E_B;

σ_{ij} *is* the doubly-differential inclusive cross section for the production of type-i particles with energy E and a direction $\vec{\Omega}$ from nuclear collisions or decay of type-j particles with a direction E_B and a direction $\vec{\Omega}'$; and

β_i is the velocity of a particle of type i divided by the speed of light c ;
and τ_i is the mean life of a radioactive particle of type i in the rest frame.

This equation is quite difficult to solve in general and special techniques have been devised to yield useful results. The Monte Carlo method is the most common method of solution used in the field of radiation shielding.

2.4 The Monte Carlo Method

2.4.1 General Principles of the Monte Carlo Technique

The Monte Carlo method is based on the use of random sampling to obtain the solution of the Boltzmann equation. It is one of the most useful methods for evaluating radiation hazards for realistic geometries that are generally quite difficult to characterize using

analytic techniques (i.e., with equations in closed form). The calculation proceeds by constructing a series of trajectories, each segment of which is chosen at random from a distribution of applicable processes. In the simplest and most widely used form of the Monte Carlo technique, the so-called **inverse transform method**, a **history** is obtained by calculating travel distances between collisions and then sampling from distributions in energy and angle made up from the cross sections,

$$\sigma_{ij}(E_B \rightarrow E, \vec{\Omega}' \rightarrow \vec{\Omega}) . \tag{2.10}$$

The result of the interaction may be a number of particles of varying types, energies, and directions each of which will be followed in turn. The results of many histories will be processed, leading typically to some sort of mean and standard deviation.

If $p(x)dx$ is the **differential probability** of an occurrence at $x \pm 1/2\ dx$ in the interval, $[a,b]$, then the integration

$$P(x) = \int_a^x dx' p(x') \tag{2.11}$$

gives $P(x)$, the **cumulative probability** that the event will occur in the interval $[a, x]$. The cumulative probability function is monotonically increasing with x and satisfies the conditions $P(a) = 0$, $P(b) = 1$. If a random number R is chosen, uniform on the interval [0, 1] from a computer routine, the equation

$$R = P(x) \tag{2.12}$$

corresponds to a random choice of the value of x, since the distribution function for the event $P(x)$ can, in principle, be inverted as

$$x = P^{-1}(R) . \tag{2.13}$$

As a simple illustration, to determine when an uncharged particle undergoes a reaction in a one-dimensional system with no decays ($d = 0$), no competing processes ($S = 0$), and no "in-scattering" ($Q = 0$), one notes from Eqs. (1.6, 2.6, and 2.7) that this particle satisfies a simple application of the Boltzmann equation;

$$\tilde{\mathrm{B}}\Phi = \left\{\vec{\Omega} \cdot \nabla + \sigma_i\right\}\Phi . \tag{2.14}$$

This simple situation reduces to the following, taking in this discussion σ_t to be the *macroscopic* cross section otherwise denoted by $N\sigma$ in this text;

$$\tilde{\mathrm{B}}\Phi = \frac{d\Phi}{dx} + N\sigma\Phi = 0 . \tag{2.15}$$

The solution to this equation is the familiar

$$\Phi = \Phi_0 \exp(-x/\lambda), \tag{2.16}$$

where $\lambda = 1/N\sigma$ as in Eq. (1.8). One can replace x/λ with r, the number of mean-free-paths the particle travels in the medium. The differential probability per unit mean-free-path for an interaction is given by

$$p(r) = \exp(-r), \tag{2.17}$$

$$\text{with} \quad P(r) = \int_0^r dr' \exp(-r') = -\exp(-r') \Big|_o^r = 1 - \exp(-r) = R. \tag{2.18}$$

Selecting a random number, R, then determines a depth r that has the proper distribution. Of course, identical results apply to other processes described by an exponential function such as radioactive decay. In this simple situation, it is clear that one can solve the above for r as a function of R and thus obtain individual values of r from a corresponding set of random numbers. For many processes, an inversion this simple is not be possible analytically. In those situations, other techniques exemplified by successive approximations and table look-ups must be employed.

In a Monte Carlo calculation, the next sampling process might select which of several physical processes would occur. Another sampling might choose, for instance, the scattering. Deflections by magnetic fields might be included as well as further particle production and/or decay.

The Monte Carlo result is the number of times the event of interest occurred for the random steps through the relevant processes. As a counting process it has a counting uncertainty and the variance will tend to decrease as the square root of the number of calculations run on the computer. Thus high probability processes can be more accurately estimated than low probability processes such as passage through an effective shield in which the radiation levels are attenuated over many orders of magnitude. Sophisticated techniques are employed which temporarily give enhanced probabilities to the low-probability events during the calculation in order to study them with the normal probabilities restored at the end of the calculation by removing these so-called “weights”. It is by no means clear that the distributions obtained using the Monte Carlo method will be distributed according to the normal, or Gaussian distribution, so that a statistical test of the adequacy of the mean and standard deviation may be required.

2.4.2 Monte Carlo Example; A Sinusoidal Angular Distribution of Beam Particles

Suppose one has a distribution of beam particle particles such as exhibited in Fig 2.2.

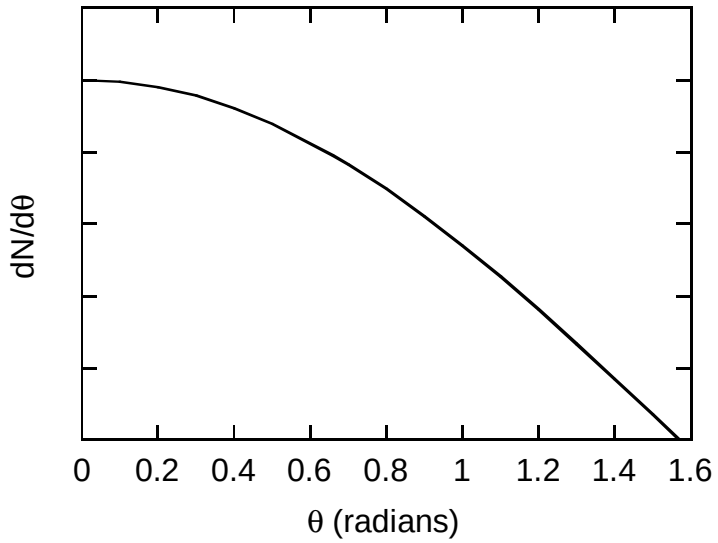

Fig. 2.2 Hypothetical angular distribution of particles obeying a distribution proportional to cos θ.

For this distribution, $p(\theta) = A \cos\theta$ for $0 < \theta < \pi/2$. Then, the fact that the integral of $p(\theta)$ over the relevant interval must be unity implies $A = 1$ since

$$P(\pi/2) = \int_0^{\pi/2} d\theta A\cos\theta = A\sin\theta \,\Big|_0^{\pi/2} \overset{\text{def}}{=} 1. \tag{2.19}$$

Thus, $p(\theta) = \cos\theta$. The cumulative probability, $P(\theta)$, is given by:

$$P(\theta) = \int_o^{\theta} d\theta' p(\theta') = \int_o^{\theta} d\theta' \cos\theta' = \sin\theta' \,\Big|_o^{\theta} = \sin\theta \ . \tag{2.20}$$

If R is a random number, then $R = P(\theta)$ determines a unique value of θ; hence:

$$\theta = \sin^{-1}(R) \ . \tag{2.21}$$

One can perform a simple Monte Carlo calculation using, for example, 50 random numbers. To do this one should set up at table such as Table 2.1 that was generated using a particular set of such random numbers. One can set up a set of bins of successive ranges of θ-values. The second column is a "tally sheet" for collecting "events" in which a random number R results in a value of θ within the associated range of θ-values. θ_{mid} is the midpoint of the bin (0.1, 0.3,...). Column 4 is the normalized number in radians found from the following:

$$N = \frac{\text{Number found in Monte Carlo bin}}{(\text{Total number of events})(\text{bin width})}$$
$$= \frac{\text{Number found in bin in Monte Carlo}}{(50)(0.2 \text{ radians})}. \quad (2.22)$$

Table 2.1 Tally sheet for Monte Carlo example.

θ (radians)	R (random #)	Total R's in Bin	N (norm. #)	cos θ_{mid}
0.0 - 0.199	~~1111~~ ~~1111~~ 1	11	1.1	0.995
0.2 - 0.399	~~1111~~ ~~1111~~ 111	13	1.3	0.955
0.4 - 0.599	~~1111~~ ~~1111~~ 1	11	1.1	0.877
0.6 - 0.799	1111	4	0.4	0.765
0.8 - 0.999	~~1111~~ 11	7	0.7	0.621
1.0 - 1.199	1111	4	0.4	0.453
1.2 - 1.399				0.267
1.4 - 1.57				0.086

One can calculate exactly the mean value of θ for the specified distribution:

$$\langle\theta\rangle = \frac{\int_0^{\pi/2} \theta\, p(\theta) d\theta}{\int_0^{\pi/2} p(\theta) d\theta} = \frac{\int_0^{\pi/2} \theta \cos(\theta) d\theta}{1} = \left[\cos\theta + \theta \sin\theta\right]_0^{\pi/2}$$
$$\langle\theta\rangle = \left[0 - 1 + \frac{\pi}{2} - 0\right] = 0.57 \quad (2.23)$$

To calculate the same quantity from the Monte Carlo result, one proceeds first by multiplying the frequency of Monte Carlo events for each eight angular bins from the table by the midpoint value of the bins. Then one sums over the 8 bins and divides by the number of incident particles (50 in this example). Thus one can determine the average value of θ, $<\theta>_{MC}$ calculated by the Monte Carlo technique:

$$<\theta>_{MC} = [(11)(0.1) + (13)(0.3) + (11)(0.5) + (4)(0.7) + (7)(0.9) + (4)(1.1)]/50 = 0.48. \quad (2.24)$$

It is easy to see from this simple example involving very coarse bins and a very small number of histories that the agreement is quite good in spite of the rather poor "statistics". This example also illustrates that the statistical errors are generally larger for the more rare events here represented by large values of θ (i.e., $\theta > 1$ radian). The choice of bin sizes is also crucial.

Practical Monte Carlo calculations generally involved the need to follow many histories. Early calculations of this type, such as the one reported by Wilson (Wi52), were made using devices such as "wheels of chance" and hand-tallying. The advent of digital computers has rendered this technique much more powerful. As the speed of computer processors has increased, the ability to model the physical effects in more detail and with ever improving statistical accuracy has resulted. In later chapters, results obtained using specific codes will be presented. Descriptions of the codes themselves, accurate as of this writing, are presented in Appendix A. The reader should be cautioned that most of these codes are being constantly improved and updated. The wisest practice in using them is to consult with the authors of the codes directly.

2.5 Review of Magnetic Deflection and Focussing of Charged Particles

2.5.1 Magnetic Deflection of Charged Particles

Particle accelerators of all types operate by utilizing electromagnetic forces to accelerate and deflect charged particles. These forces have been well described in detail by other authors such as Edwards and Syphers (Ed93), Carey (Ca87), and Chao and Tigner (Ch99). In accelerator radiation protection, an understanding of these forces is motivated by the need to be able to determine the deflection of particles by electric or magnetic fields. Clearly, one needs to be able to assure that particles in a deflected particle beam either interact with material where such interactions are desired or avoid such points of beam loss. The answers to such questions are interconnected with the design of the accelerator and, for those purposes, advanced texts such as those cited above should be consulted. This is especially true for situations involving the application of radiofrequency (RF) electromagnetic fields to the particle beams where a full treatment using electrodynamics is needed. However, some of the issues are quite simple and are discussed in this section.

The force, $\vec{F}$ (Newtons) on a given charge, q (Coulombs), at any point in space is given, in SI units, by

$$\vec{F} = q(\vec{v} \times \vec{B} + \vec{E}) = \frac{d\vec{p}}{dt}, \tag{2.25}$$

where the electric field, $\vec{E}$, is in Volts meter^{-1}, the magnetic field $\vec{B}$ is in Tesla (1 Tesla = 10^4 Gauss), and $\vec{v}$ is the velocity of the charged particle in km sec^{-1}, $\vec{p}$ is the momentum of the particle in SI units, and t is the time (sec). The direction of the force due to the cross product in Eq (2.25) is, of course, determined by the usual **right-hand** rule. Static electric fields (i.e., $d\vec{E}/dt = 0$), if present, serve to accelerate or decelerate the charged particles. In a uniform magnetic field without the presence of an electric field, due to

the cross product in this equation, any component of $\vec{p}$ which is parallel to $\vec{B}$ will not be altered by the magnetic field. Typically, charged particles are deflected by dipole magnets in which the magnetic field is, to high order, spatially uniform and constant in time, or slowly-varying compared with the time during which the particle is present. For this situation, if there is no component of $\vec{p}$ which is parallel to $\vec{B}$, the motion is circular and the magnetic force serves to supply the requisite centripetal acceleration. The presence of a component of $\vec{p}$ which is parallel to $\vec{B}$ results in a trajectory that is a spiral rather than a circle. Figure 2.3 illustrates the condition of circular motion. Equating the centripetal force to the magnetic force and recognizing that $\vec{p}$ is perpendicular to $\vec{B}$ leads to

$$\frac{mv^2}{R} = qvB, \tag{2.26}$$

where m is the *relativistic* mass (see Eq. 1.11). Solving for the radius of the circle, R (meters), recognizing that $p = mv$, and changing the units of measure for momentum, one gets

$$R(\text{meters}) = \frac{p}{qB}\ (\text{SI units}) = \frac{p(\text{GeV/c})}{0.29979qB}, \tag{2.27}$$

where q in the denominator of the right hand side is now the *number* of electronic charges carried by the particle and B remains expressed in Tesla. The numerical factor in the denominator is just the mantissa of the numerical value of the speed of light in SI units.

In practice, at large accelerators, one is often interested in the angular deflection of a magnet of length, L, which provides such a uniform field orthogonal to the particle trajectory. Such a situation is also shown in Fig. 2.3. If L is only a small piece of the complete circle (i.e., $L << R$), one can consider the circular path over such a length to be two straight line segments. Doing this, one finds that the change in direction, $\Delta\theta$, is given by

$$\Delta\theta = \frac{L}{R} = \frac{0.29979qBL}{p}\ (\text{radians}), \tag{2.28}$$

where the product, BL (Tesla-meters) is commonly referred to the **field integral** of the magnet system and p remains in GeV/c. It is evident that BL could just as well be obtained by integrating a non-uniform field over the length of the magnet system. This angle of deflection can be used to deduce if the particle beam will, or will not, interact with some solid object near its path, a matter of practical importance for radiation protection.

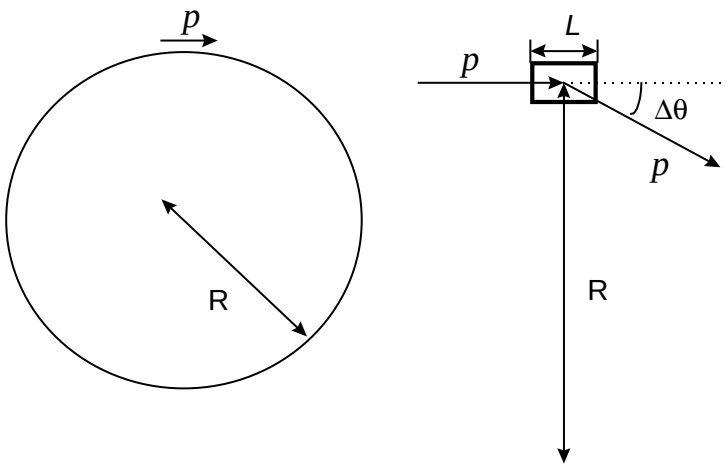

Fig. 2.3 A particle of positive charge q having momentum $\vec{p}$ follows a circular path when directed perpendicular to a static, uniform magnetic field $\vec{B}$. The figure on the left illustrates this for a complete circle. On the right, a particle of momentum $\vec{p}$ enters a magnet of length L that has field integral value of BL. For this example, $L << R$ and the particle experiences a small angular deflection $\Delta\theta$. The angular deflection is exaggerated in this figure for clarity.

2.5.2 Magnetic Focussing of Charged Particles

Now we consider, in a simplified way, how the focussing of charged particle beams can be accomplished using of quadrupole magnets. Edwards and Syphers (Ed93) and Carey (Ca87) describe in much more detail the magnetic deflections in general electromagnetic systems, including quadrupole magnets, and those of higher order which focus particle beams. Mathematical methods analogous to those found in the study of geometric optics are often used to describe the optics of charged particles. Where time-varying electric and magnetic fields are involved, the full complement of Maxwell's equations must, of course, be used to describe the motion of charged particles. The application of higher order multipole fields and the employment of radiofrequency ("RF") electromagnetic fields to accelerate, decelerate, and otherwise manipulate charged particle beams is left to the specialized texts.

An idealized quadrupole magnet has the transverse cross section shown in Fig. 2.4, which also defines the Cartesian coordinate system to be used in the remainder of this section. As one can see, the polarities of the pole pieces alternate. Following the usual convention, the longitudinal coordinate, z, is taken to be directed along the beam and, in this case, "into the paper" along the **optic axis** of the quadrupole. Positive values of the y-coordinate measure upward deviations from the optic axis while positive values of the x-coordinate measure deviations from the optic axis to "beam left", to maintain consistency with the familiar **right hand rule**.

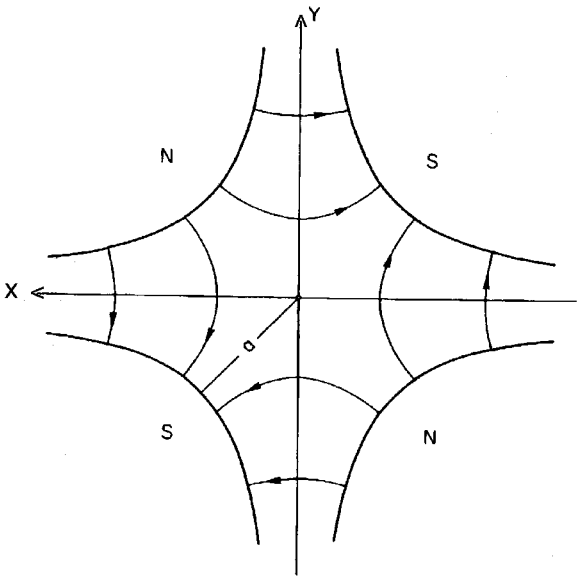

Fig. 2.4 Cross section of a typical quadrupole magnet. The pole pieces are of opposite magnetic polarities, denoted "N" and "S", and are of hyperbolic shapes. A Cartesian coordinate system is used in which *x* and *y* denote transverse coordinates while *z* is along the desired beam trajectory, the optic axis of the beam optical system. In this figure, the beam enters the quadrupole into the paper along the positive *z* axis. The curves with arrows denote magnetic field lines. [Adapted from (Ca87).]

Often in the accelerator magnets themselves and nearly always in beam lines transmitting extracted particles, the electromagnetic fields vary only slowly with time or are static compared with the particle transit times. Under these conditions, it is shown in other texts that if the shape of the pole pieces are hyperbolae described by equations of form $xy = \pm k$, and if the pole pieces are uniformly magnetized, then the components of the magnetic field within the gap containing the beam are given by:

$$B_x = -\frac{B_o}{a} y = -gy \text{ , and} \tag{2.29a}$$

$$B_y = -\frac{B_o}{a} x = -gx \text{ .} \tag{2.29b}$$

Here, a is the gap dimension as defined in Fig. 2.4 and B_o is the magnitude of the magnetic field strength at the pole pieces. The parameter g is, quite naturally, called the **gradient** of the quadrupole. This configuration defines an ideal quadrupole, which is of length, L.

Now examine qualitatively what happens to a particle having positive charge that enters this magnet parallel to the *z*-axis. If the particle trajectory is along the optic axis, then it

will not be deflected at all since $B_x = B_y = 0$. If, however, the particles enter the magnet parallel to the optic axis but with some finite *positive* value of *y*, it will receive a deflection toward *smaller* values of *y* in accordance with the right hand rule and Eq. (2.25). Likewise, if it enters with a finite *negative* value of *y*, it will receive a deflection toward *less negative* values of *y*. Thus, a beam of such particles is said to be **focussed** in the *yz* plane. However, if the particle enters with a finite positive value of *x*, it will be deflected toward a *larger* value of *x*, away from the optic axis. Finally, a particle incident with a finite negative value of *x* will similarly be deflected away from the optic axis. Thus, a beam of such particles is said to be **defocussed** in the *xz* plane. From this qualitative discussion it should be clear that more than one quadrupole will be needed to achieve a net focussing effect.

Considering just the situation in the *yz* plane, it is easy to see that the analogy with geometrical optics goes further. For a particle entering with coordinate *y*, one can substitute into Eq (2.28) and find that the angular deflection, if small compared with the dimensions of the magnet, is given by:

$$\Delta\theta = \frac{0.29979qLgy}{p} \text{ (radians)}, \tag{2.30}$$

where the same units as Eq. (2.28) have been employed, with *g* (Tesla meter^{-1}) and *y* (meters) inserted. If the incident particle trajectory is parallel with the *z*-axis, the situation is schematically shown in Fig. 2.5a. In schematic drawings of beam optics, it is customary to show convex lenses to denote focussing elements and concave lenses to represent defocussing elements pertinent to a given plane. Bending magnets are correspondingly represented by prisms in such drawings.

Applying simple trigonometry, one finds that after deflection in this situation, the particle trajectory will intercept the *z*-axis at a distance, *f*, given as follows,

$$f = \frac{y}{\tan\Delta\theta} \approx \frac{y}{\Delta\theta} = \frac{p}{0.29979qLg}, \tag{2.31}$$

since the deflection, $\Delta\theta$, is small. This approximation is called the **thin lens** approximation. In recognition of the fact that *f* is independent of the *y* coordinate, it is called the **focal length** of the quadrupole. By analogy with optical thin lenses, one can write down **the thin lens equation** which gives the relationship between the image distance, z_i, and the object distance, z_o, for other rays as follows,

$$\frac{1}{z_o} + \frac{1}{z_i} = \frac{1}{f}. \tag{2.32}$$

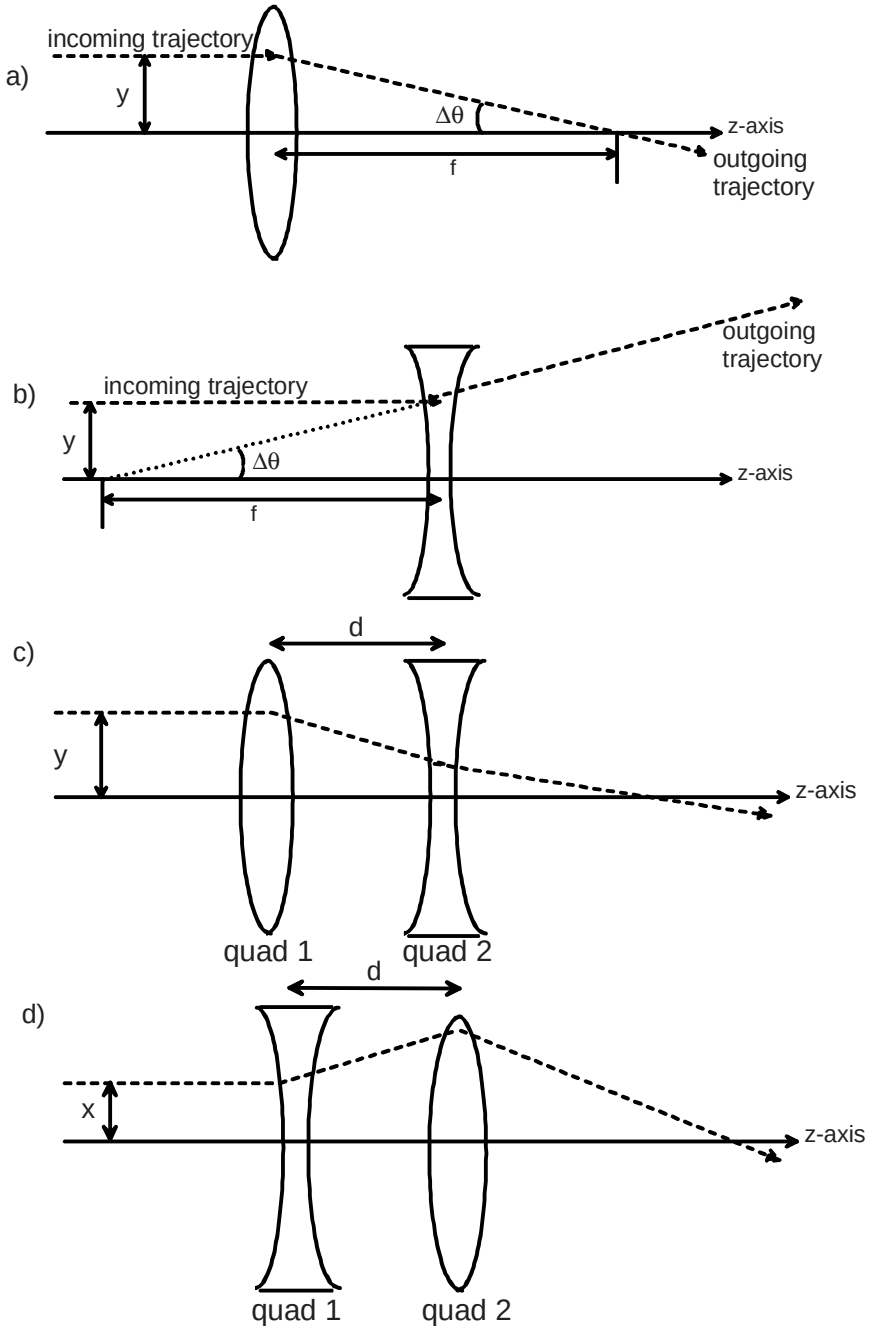

Figure 2.5 Configurations of quadrupole lenses: **a)** Representation of focusing in the *yz* plane of a beam trajectory incident from the left parallel to the *z*-axis. The notation is explained in the text. A *real* image is formed at the focal length, *f*, from the lens. **b)** Representation of defocusing in the *yz* plane. The parallel beam is deflected so that it appears to emerge from a point a distance *f* before the lens, thus, forming a *virtual* image. **c)** Representation of a particle trajectory in the *yz* plane of a quadrupole doublet. The particle enters a quadrupole doublet parallel to the *z*-axis from the left. First a focusing quadrupole (quad 1) is encountered and then a defocussing quadrupole (quad 2) follows. **d)** Representation of a particle trajectory in the *xz* plane of the same doublet. The particle enters the doublet parallel to the *z*-axis. In this plane, the defocussing quadrupole is encountered first.

In this equation, z_o and z_i are > 0 if the object is to the left of the lens and the image is to the right of the lens, forming a *real* image, for a focussing lens with $f > 0$. The situation for the defocussing plane, here the *xz* plane, is shown in Fig. 2.5b as a concave lens. For that plane, the equations are still workable if one applies a negative sign to the value of *f* and understands that a value of $z_i < 0$ describes a *virtual* image.

The simplest configuration of quadrupole magnets is in the form of a pair of two such magnets. In a given plane, say the *yz*, the first would be focussing while the second would be defocussing. In the orthogonal plane, here the *xz*, the defocussing quadrupole would thus be encountered first. Generally, these magnets will be of identical dimensions and have gradients of similar magnitudes. Such a **quadrupole doublet** is shown in Figs 2.5c and 2.5d for the *yz* and *xz* planes, respectively.

Eq. (2.32) can now be employed to explore how a quadrupole doublet can focus a parallel beam in both the *xz* and *yz* planes in a simple example. For the sake of this discussion, the quadrupoles, quad 1 and quad 2, have different focal lengths, f_1 and f_2, respectively, and are separated by distance *d*. Quad 1 is focussing in the *yz* plane. As one would do in geometrical optics, for an incoming parallel beam, the object distance relative to quad 1 is $z_{yo1} \rightarrow \infty$. Thus, the image distance from quad 1 is at $z_{yi1} = f_1$. The object distance of this image from quad 2 is thus $z_{yo2} = d - f_1$. Relative to quad 2, the location of the final image will be at z_{yi2} by means of the thin lens equation,

$$\frac{1}{z_{yi2}} = \frac{1}{-f_2} - \frac{1}{d - f_1}, \tag{2.33}$$

where the negative coefficient of f_2 explicitly recognizes that lens 2 is *defocussing* in the *yz* plane. Solving,

$$z_{yi2} = \frac{f_2(f_1 - d)}{f_2 - f_1 + d}. \tag{2.34a}$$

If the quadrupoles are identical ($f = f_1 = f_2$), then,

$$z_{yi2} = \frac{f\ (f - d)}{d}. \tag{2.34b}$$

It is simple to follow the same procedure for the *xz* plane to obtain the corresponding image distance, z_{xi2},

$$z_{xi2} = \frac{f_2(f_1 + d)}{f_1 - f_2 + d}. \tag{2.35a}$$

With identical quadrupoles, this becomes,

$$z_{xi2} = \frac{f\ (f+d)}{d}. \tag{2.35b}$$

One should notice that with identical quadrupoles,

$$z_{xi2} - z_{yi2} = 2f\ , \tag{2.36}$$

a result that should not be surprising given that particles in *xz* plane are first subject to *defocussing*, and thus become more divergent, prior to their being focussed. The average focal length of the system for both the *xz* and *yz* planes is thus f^2/d. More sophisticated schemes such as quadrupole triplets and non-identical magnets can be used, where needed, to obtain a specialized beam envelope. These advanced methods are discussed in great detail, for example, by Carey (Ca87).

In this simple exposition, a number of significant effects have been ignored. First, a typical particle beam will contain some spread in particle momenta. The derivation given above ignores the fact that **dispersion** will occur in the magnetic fields in the same way that prism disperses a visible beam of "white" light into the various colors. There also may be **aberrations** or distortions of an image. One such aberration is analogous to **chromatic aberration** encountered in geometrical optics. Furthermore, the fact that no particle beam is ever completely parallel or completely emergent from a geometrical point has been ignored.

All particle beams possess a property called **transverse emittance**. This quantity is expressed in units of angular divergence times physical size, typically in units of π mm-mradian. The explicit display of the factor π is a matter of custom. The emittance concept is used to describe both longitudinal and transverse phenomena and is discussed by Carey (Ca87) and by Edwards and Syphers (Ed93). The discussion here is limited to transverse emittance. During the process of accelerating particles, the beam emittance in general becomes smaller because the normalized transverse emittance [the emittance when multiplied by the relativistic factors $\gamma\beta$ from Eqs. (1.10) and (1.11)] is an invariant. Thus, as velocity increases, the unnormalized emittance must decrease since the product $\gamma\beta$ increases with particle momentum. There are exceptions to this generalization beyond the scope of this discussion. Once a beam is no longer subject to RF fields in an accelerator, the emittance can generally no longer be made smaller and can only increase due to processes such as multiple Coulomb scattering, space charge effects, etc.[3] Under conditions in which the emittance is approximately constant, the product of the angular divergence of the beam envelope and the size of the beam envelope is conserved, as it

[3] Under some conditions not discussed further here, synchrotron radiation can, in fact, reduce the transverse emittance.

must by Liouville's theorem. This means that efforts made to focus the beam tightly into a small size will unavoidably result in a beam with a correspondingly larger angular spread. Likewise, attempts to create a parallel beam (one with essentially no angular spread) will result in a correspondingly larger beam size.

As a final word, one should be aware of the fact that the above discussion of quadrupoles depends upon the beam axis coinciding with the optic axis. Should the beam enter a quadrupole with its center far off-axis, it should be obvious that the entire beam will be deflected nearly as if a quadrupole were a dipole magnet of equivalent field strength and length (see Fig. 2.4). Beams that are deflected in this manner by a quadrupole are said to have suffered **steering**. The steering of beams can constitute significant loss points in the beam transport system.

Problems

1. This problem gives two elementary examples of Monte Carlo techniques that are almost "trivial". In this problem, obtaining random numbers from a standard table or from a hand calculator should be helpful.

   a) First, use a random number table or random number function on a calculator along with the facts given about the cumulative probability distribution for exponential attenuation to demonstrate that, even for a sample size as small as, say, 15, the mean value of paths traveled is "within expectations" if random numbers are used to select those path lengths from the cumulative distribution. Do this, for example, by calculating the mean and standard deviation of your distribution.

   b) An incident beam is subjected to a position measurement in the coordinate *x*. It is desirable to "recreate" incident beam particles for a shielding study using Monte Carlo. The *x* distribution as measured is as follows:

x	**#**
0	0
1	1
2	2
3	3
4	4
5	5
6	4
7	3
8	2
9	1
10	0

   Determine, crudely, *p(x)*, *P(x)* and then use 50 random numbers to "create" particles intended to represent this distribution. Then compare with the original one which was measured in terms of the average value of *x* and its standard deviation. Do <u>not</u> take the time to use interpolated values of *x*, simply round off to integer values of *x* for this demonstration.

2. A beam of protons having a kinetic energy of 100 GeV is traveling down a beam line. The beam is entirely contained within a circle of diameter 1 cm. All of the beam particles have the same kinetic energy. An enclosure further downstream must be protected from the beam or secondary particles produced by the beam by shielding it with a large diameter iron block that is 20 cm in radius centered on the beam line. The beam passes by this block by being deflected by a uniform field magnet that is 3 meters long and is located 30 meters upstream of the iron block. Calculate the magnetic field, *B*, that is needed to accomplish this objective.